

X-910-75-80

PREPRINT

NASA TM X-70867

# BEAUFORT SEA ICE ZONES BY MEANS OF MICROWAVE IMAGERY

ORIGINAL CONTAINS  
COLOR ILLUSTRATIONS

P. GLOERSEN  
W. J. CAMPBELL  
R.O. RAMSEIER  
W. J. WEBSTER  
T. T. WILHEIT



APRIL 1975

N75-20967

Unclas  
18175

G3/48

(NASA-TM-X-70867) BEAUFORT SEA ICE ZONES BY  
MEANS OF MICROWAVE IMAGERY (NASA) 27 P. HC  
\$3.75 CSCL 08L



— GODDARD SPACE FLIGHT CENTER —  
GREENBELT, MARYLAND

For information concerning availability  
of this document contact:

Technical Information Division, Code 250  
Goddard Space Flight Center  
Greenbelt, Maryland 20771  
(Telephone 301-982-4488)

"This paper presents the views of the author(s), and does not necessarily  
reflect the views of the Goddard Space Flight Center, or NASA."

BEAUFORT SEA ICE ZONES BY  
MEANS OF MICROWAVE IMAGERY

W. J. Campbell  
P. Gloersen  
R. O. Ramseier  
W. J. Webster  
T. T. Wilhelm

GODDARD SPACE FLIGHT CENTER  
Greenbelt, Maryland

BEAUFORT SEA ICE ZONES BY  
MEANS OF MICROWAVE IMAGERY

W. J. Campbell

P. Gloersen

R. O. Ramseier

W. J. Webster

T. T. Wilheit

INTRODUCTION

During June 1970, March-April 1971, and April 1972 the NASA CV-990 research aircraft obtained extensive imagery and photography of the sea ice in the Beaufort Sea in conjunction with the three Arctic Ice Dynamics Joint Experiment (AIDJEX) pilot experiments. These data (Wilheit et al, 1972; Gloersen et al, 1973; Campbell et al, 1974) have shown that a wide variety of morphological and dynamical ice features can be observed by aircraft remote sensing and also found that data needed in developing and testing numerical models of the ice pack can be acquired by aircraft. These data also are of great aid in the interpretation of satellite images of sea ice, i. e., the high-resolution visible imagery obtained by LANDSAT-1 and the all-weather, day or night microwave imagery obtained by the ESMR (Electrically Scanning Microwave Radiometer) on NIMBUS-5.

In this paper, a more detailed analysis of some of the aircraft microwave data obtained during the AIDJEX 1972 pilot experiment is presented and compared with a recent analysis of the microwave brightness temperatures measured in situ in the vicinity of the main AIDJEX camp (Meeks et al, 1974).

During April 1972, microwave and infrared data were obtained from the NASA CV-990 research aircraft over the Beaufort Sea ice from the shoreline of Harrison Bay northward to the AIDJEX experiment area (at an approximate latitude of  $75^{\circ}\text{N}$  and longitude of  $150^{\circ}\text{N}$ ) and north of the test area up to a latitude of almost  $81^{\circ}\text{N}$ . Over this north-south transect of the polar ice canopy, it was discovered that the sea ice could be divided into five distinct zones. The properties of each will be discussed in some detail below. Briefly, they are as follows:

(1) First Zone: The shorefast sea ice, which will be referred to as the shorefast zone, was found to consist uniformly of first-year sea ice.

(2) Second Zone: A mixture of first-year sea ice, medium-size multiyear floes, and considerable thin ice and open water, which will be called the shear zone.

(3) Third Zone: A mixture of first-year and multiyear sea ice which has a uniform microwave signature because the multiyear ice floes are smaller than the instantaneous field-of-view (IFOV) of the airborne radiometer.

(4) Fourth Zone: A mixture of first-year sea ice and medium to large size multiyear floes which is similar in composition to the shear zone (second zone).

(5) Fifth Zone: Almost exclusively multiyear ice extending to the North Pole, which will be called the polar ice zone.

#### OBSERVATION METHOD

The aircraft used in these studies was the NASA CV-990, which contained the complement of microwave, infrared, and photographic instruments listed in Table 1. The radiometric data were digitized and recorded in digital form on magnetic tape. Table 2 lists the seven aircraft flights made during the experiment. From the Alaskan coast up to a latitude of  $74^{\circ}\text{N}$  each of the seven missions was flown along the same meridians permitting formation of two parallel-track mosaic of the photographic and microwave data. These mosaics permitted observations of the ice dynamics and morphology between the coast and the AIDJEX area. The 100 km by 100 km remote sensing test area was always located so that the main AIDJEX camp area was near the southeast corner. In this way photomosaics and microwave image mosaics were obtained of the nearly same ice area each time which always included areas in which surface observations were being made during each flight. Since there was a general westward drift of the AIDJEX array averaging 6 km per day, the aircraft paths between  $74^{\circ}\text{N}$  and  $75^{\circ}\text{N}$  varied from one flight to the next. The flights were arranged to coincide with periods of pronounced ice dynamic activity in the AIDJEX area. In particular, the goal was to obtain flights soon before and soon after the passage of cyclones near the test area. On one occasion, a

four parallel track pattern was flown so that the microwave mosaic could be extended from 75°N (near the main AIDJEX camp) to 80° 45'N. The altitude flown for most of these missions was 11 km. On one occasion, a 14 track grid was flown at an altitude of 3 km to obtain a microwave image with higher spatial resolution.

## SEA ICE ZONES

Line tracings of the radiometric brightness temperatures at wavelengths of 0.8 cm and 1.55 cm from the north coast of Alaska up to 80° 45'N obtained in early April 1972 are shown in Figure 1. It can be seen that the shorefast zone (zone 1) is typified by uniformly high brightness temperatures, except for an open lead encountered about 25 km north of the shoreline. The shear zone (zone 2) generally displays as low a brightness temperature as for any sea ice type but also shows strong fluctuations. The average brightness temperature in zone 3 is between that of zones 1 and 2, and while reasonably uniform in appearance it still shows greater fluctuation than observed in zone 1. The boundaries of zone 4 are less distinct than those of the shear zone (zone 2) which has a similar composition, but the average brightness temperature of each zone is similar. The brightness temperature of the polar ice zone (zone 5) approaches a uniform low value.

As can be seen in Figure 1, the radiometric signature of each ice zone is more pronounced at 0.8 than at 1.55 cm. In fact, at the longest wavelengths (2.8 cm and longer) the signatures (not shown) were observed to become less and less distinguishable.

### Zone 1

In Figure 2, the data obtained by the 1.55 cm microwave imager are given in false-color format for each of the seven flights from the north shoreline of Alaska (Harrison Bay) to a latitude 74°N on the Beaufort Sea ice canopy.



The shorefast ice shows a brilliant solid red color corresponding to a brightness temperature near  $250^{\circ}\text{K}$ . The brightness temperature is remarkably uniform within this band with the exception of occasional large open leads which lower the brightness temperatures. Also, the open lead signatures disappear on subsequent flights leaving no indication of their previous occurrence. It is interesting to note that the brightness temperature of this uniform ice is essentially identical to the brightness temperature of refrozen polynyas in the other test areas. Surface measurements were made at Harrison Bay and Kogru River on 25 April 1972 to obtain physical properties of the shorefast ice. It was found that the shorefast ice, as expected, was entirely first-year ice covered by an average of 0.18 m of snow. The surface relief varied between 0.14-0.25 m giving the snow cover a wavelike appearance. Physical properties of typical ice samples from Harrison Bay and Kogru River are illustrated in Figure 3.

Another notable property of the shoreline ice is its gradual reduction in extent over the 20-day period of the experiment. As Figure 2 shows, it became approximately 30 km narrower in that period of time.

### Zone 2

Referring again to Figure 2, it can be seen that zone 2, the shear zone, is clearly delineated at both its southern and northern boundaries. Also, the width of zone almost doubles over the 20-day period of the flights as the ice flows westward. Three distinct form of ice appear: (1) There are large floes depicted by the cool radiometric signatures (blue) which are multiyear ice floes.

The partially resolved open leads that occur also give a similar brightness temperature due to a combination of the radiometrically cold water signature, and the warm ice signature but they can be recognized by their lineal nature.

(2) There are refrozen leads and polynyas with a warm brightness temperature similar to that of the shorefast ice. (3) Finally, there is the ice represented in the images as yellow, which is interpreted as a mixture of first-year ice and unresolvable chunks of multiyear ice. The transport of ice and refrozen polynyas through the area of the CV-990 flight paths can be measured from the successive microwave images. Figure 4 is a vector diagram showing the complex ice flow deduced by tracking recognizable ice features in the microwave images. The motion averages about 4 km a day to the west, although the motions are complicated by the alternating anticyclonic-cyclonic activity over the area during this period. This is somewhat lower than the average westward drift motion observed at the main AIDJEX camp (about 6 km per day) over the 20-day interval of the aircraft flights.

### Zone 3

An early attempt (Campbell et al, 1974) was made to identify the nature of sea ice in the 100 km x 100 km AIDJEX '72 test area (which was in the third zone) from the aircraft radiometric data alone. Based on the uniform brightness temperatures in the test area, earlier evidence from the 1971 AIDJEX data (Gloersen et al, 1973), and lack of information on the scattering coefficient for

the snow and the temperature dependence of the emissivity of the sea ice, it was concluded that the test area consisted largely of first-year sea ice, perhaps as much as 85%. As a result of the higher resolution surface measurements (Meeks et al, 1974) by ground-based microwave radiometers, it was found that a much smaller 110 m x 110 m test area in the immediate vicinity of the main AIDJEX camp consisted both of first-year ice and small multiyear pieces of the order of ten meters in diameter. The percentage of multiyear ice in this smaller test area was 59% (Meeks et al, 1974). The aircraft radiometer, however, was only able to resolve multiyear pieces 500 meters or greater in extent from its normal flight altitude of 11 km. In fact, more small multiyear floes (approximately 150 meters in extent or more) could be distinguished in the data obtained from the 3 km altitude test pattern (see Table 2), but the total area of these small floes was well under 59% of the total field of view. When the brightness temperature variations obtained on the surface are averaged, the surface-based radiometer readings agree with those obtained from the aircraft. Since this small area appeared to be typical of the ice within the larger AIDJEX test area, and since its average brightness temperature agrees with that of the area observed by aircraft, the ice of the third zone is probably composed of approximately equal amounts of first-year and small multiyear ice floes.

The drift tracks obtained by navigational satellite positioning of the three AIDJEX '72 campsites are given in Figure 5. It can be seen that the average drift is about 6 km per day, with surges occurring during and shortly

after cyclone passages in nearby areas. The deformations that took place within the test area have been measured accurately by means of laser ranging and has been discussed elsewhere (Weeks et al, 1973). The absence of sufficiently large multiyear ice floes and well-defined refrozen leads within zone 3 prevented the deduction of the flow pattern from successive microwave images as was done for zone 2. Certain large refrozen polynya features, however, were noted near the main camp area and could be followed in the general westward drift of the test area. One such refrozen polynya, illustrated in Figure 6, was observed throughout the seven test days at about the same location in the image. Note that the images were geographically shifted to keep the main camp at approximately the same position in the image.

#### Zone 4

The decision to carry out observations north of the AIDJEX test area was made as a result of reviewing early microwave mosaics of the AIDJEX test area. The conspicuous absence of resolvable multiyear floes in the AIDJEX area at the same latitude where very large (50 km diameter) multiyear floes were observed to the east a year earlier (Gloersen et al, 1973) led to the decision to fly a long transect deep into the Beaufort Sea gyre to locate the multiyear ice. The 1.55 cm microwave mosaic shown in Figure 7 was obtained on this flight. It covers a large area of the ice canopy, starting at the southern edge of the AIDJEX area and continuing to 80° 45'N latitude. The first resolvable

multiyear floes appeared at approximately  $76^{\circ} 45'N$ . A mixture of first year and multiyear floes similar to that of zone 2 (shear zone) was present and continued up to  $79^{\circ}N$ . The similarity of zone 4 to zone 2 is further implied by the appearance of numerous refrozen polynyas. Although zone 4 was not mapped on each of the seven CV-990 flights during this period, it was partially observed on other missions during aircraft turns after each leg over the AIDJEX area. Visual observations therefore extended over the southern half of zone 4 during most flights, and revealed that the ice in the area was constantly undergoing deformations stronger than those observed in zone 3. Although zones 4 and 2 were alike in morphology and also appeared to be the most active of the five zones, in the absence of any models which would predict a shear zone at this latitude we hesitate to call Zone 4 a second shear zone.

#### Zone 5

The fifth and northernmost ice zone observed was made up almost exclusively of multiyear ice floes. Figure 6 shows that north of  $79^{\circ}N$  Latitude, the ice canopy was almost exclusively multiyear ice floes. The largest floes observed were several kilometers in diameter, an order of magnitude smaller than the multiyear ice floes observed in the eastern Beaufort Sea during the 1971 AIDJEX experiment and subsequent satellite studies (Ramseier et al, 1974). The variation of the size and distribution of ice floes in the Beaufort Sea and the

observed ice dynamics during the 1971 and 1972 AIDJEX experiment has been discussed earlier (Campbell et al, 1974). It was found that all microwave observations made during these experiments and later observations from the NIMBUS-5 satellite (Gloersen et al, 1974) indicate that, as one proceeds northward from any point on the southern shore of the Beaufort Sea, once the predominantly multiyear ice (Zone 5) begins it continues up to the pole with only minor variations in the ratio of multiyear to first-year ice.

## CONCLUSION

The five zones of the sea ice discussed existed in the Beaufort Sea during April 1972. They are certainly not steady-state features of the sea ice cover in that region. Extreme seasonal variations are well known historically (i. e. by the time of the fall freeze, the only remaining ice is multiyear). However, the five-zone distribution is probably a recurring feature of the late fall, winter, and spring ice cover of the region. The NIMBUS-5 Electrically Scanned Microwave Radiometer (ESMR) has been providing synoptic 1.55 cm wavelength microwave images of this region since the December 1972 launch. Campbell et al, (1974) and Gloersen et al, (1974) give winter and spring 1973 images of the Beaufort Sea ice cover in which zones 3, 4 and 5 above can clearly be seen. Figure 7 shows an ESMR image of the Arctic for December 1973 in which zones 3, 4 and 5 can also be clearly distinguished. Since the resolution of the NIMBUS-5 ESMR is only 30 km, zones 1 and 2 are difficult to recognize in the

ESMR images because the zones have widths that are only one or two resolution cells in size. A similar zonal structure is also seen in the Kara, Laptev, and East Siberian Seas.

## REFERENCES

- Campbell, W. J., P. Gloersen, W. Nordberg, and T. T. Wilheit, Dynamics and Morphology of Beaufort Sea Ice Determined from Satellites, Aircraft and Drifting Stations, Proceedings of the Symposium on Approaches to Earth Survey Problems Through Use of Space Techniques (COSPAR), (Akademie-Verlag-Berlin, 1974).
- Gloersen, P., W. Nordberg, T. J. Schmugge, T. T. Wilheit and W. J. Campbell, Microwave Signatures of First-Year and Multiyear Sea Ice, J. Geophys. Res. 78, 3564 (1973).
- Gloersen, P., T. T. Wilheit, T. C. Chang, W. Nordberg, and W. J. Campbell, "Microwave Maps of the Polar Ice of Earth," Bul. Am. Met. Soc. 55, 1442 (1974).
- Hibler III, W. D., W. F. Weeks, S. Ackley, A Kovacs and W. J. Campbell, Mesoscale Strain Measurements on the Beaufort Sea Pack Ice (AIDJEX, 1971), J. Glaciol. 12, 187 (1973).
- Weeks, D. C., R. O. Ramseier and W. J. Campbell, "A study of microwave emission properties of sea ice -- AIDJEX 1972" Proc. 9th Int. Symposium on Remote Sensing of Environment, Ann Arbor, Mich., Oct. 1974.



Ramseier, R. O., W. J. Campbell, W. F. Weeks, L. D. Arsenault, K. L.

Wilson, "Ice dynamics in the Canadian Archipelago and adjacent Arctic Basin as determined by ERTS-1 observation," Proceedings International Symposium on Canada's Continental Margins and Offshore Petroleum Exploration, Calgary, October 1974.

Wilheit, T. T., W. Nordberg, J. Blinn, W. J. Campbell and A. Edgerton,  
Aircraft Measurements of Microwave Emission from Arctic Sea Ice,  
Remote Sensing of Environment 2, 129-139 (1972).

Table 1

Instrument	IFOV	View Angle (from Nadir)	Sensitivity ( $\Delta T_{\text{RMS}}$ )
21 cm radiometer	15°	0°	0.5°K
6.0 cm radiometer	5°	38°	1°K
2.8 cm radiometer	7°	38°	1.5°K
1.55 cm scanner	2.8°	+50° to -50° cross-track	1.5°K
0.81 cm radiometer	5°	38°	3.5°K
10 $\mu\text{m}$ radiometer	<1°	0°	<1°K
RC-8 camera	73°	0°	N. A.
70 mm camera	73°	0°	N. A.

Table 2

Date	AIDJEX Grid Size (km)	Altitude (km)	# Tracks	Pattern Centered Over
4-4-72	130x130	10	10	75.7°N, 150.0°W
4-7-72	65x65	3	14	75.1°N, 148.7°W
4-12-72	130x130	10	10	75.7°N, 151.0°W
4-15-72	130x130	10	10	75.7°N, 152.7°W
4-18-72	60x640	11.3	4	77.9°N, 151.2°W
4-21-72	130x130	11.3	6	75.7°N, 153.3°W
4-23-72	130x130	11.3	8	75.7°N, 153.3°W

## FIGURES

- Figure 1: 37 GHz and 19 GHz traces of microwave brightness temperature of sea ice observed from the north coast of Alaska to  $80^{\circ}45'N$  over the western Beaufort Sea in April 1972.
- Figure 2: Successive 19 GHz microwave brightness temperature mosaic images of the sea ice cover of the western Beaufort Sea (Harrison Bay to  $74^{\circ}N$ ), April 1972.
- Figure 3: Physical Properties of Zone 1 Ice.
- Figure 4: Ice floe trajectories deduced from the successive microwave mosaic images shown in Figure 2. Unlabelled numbers refer to dates in April 1972.
- Figure 5: Drift of three AIDJEX camps.
- Figure 6: Microwave mosaic image of the sea ice from the AIDJEX area to  $80^{\circ}45'N$  for 18 April 1972.
- Figure 7: ESMP image of the Arctic on December 11, 1973.

# BEAUFORT SEA ICE LATITUDE

70 71 72 73 74 75 76 77 78 79 80 81

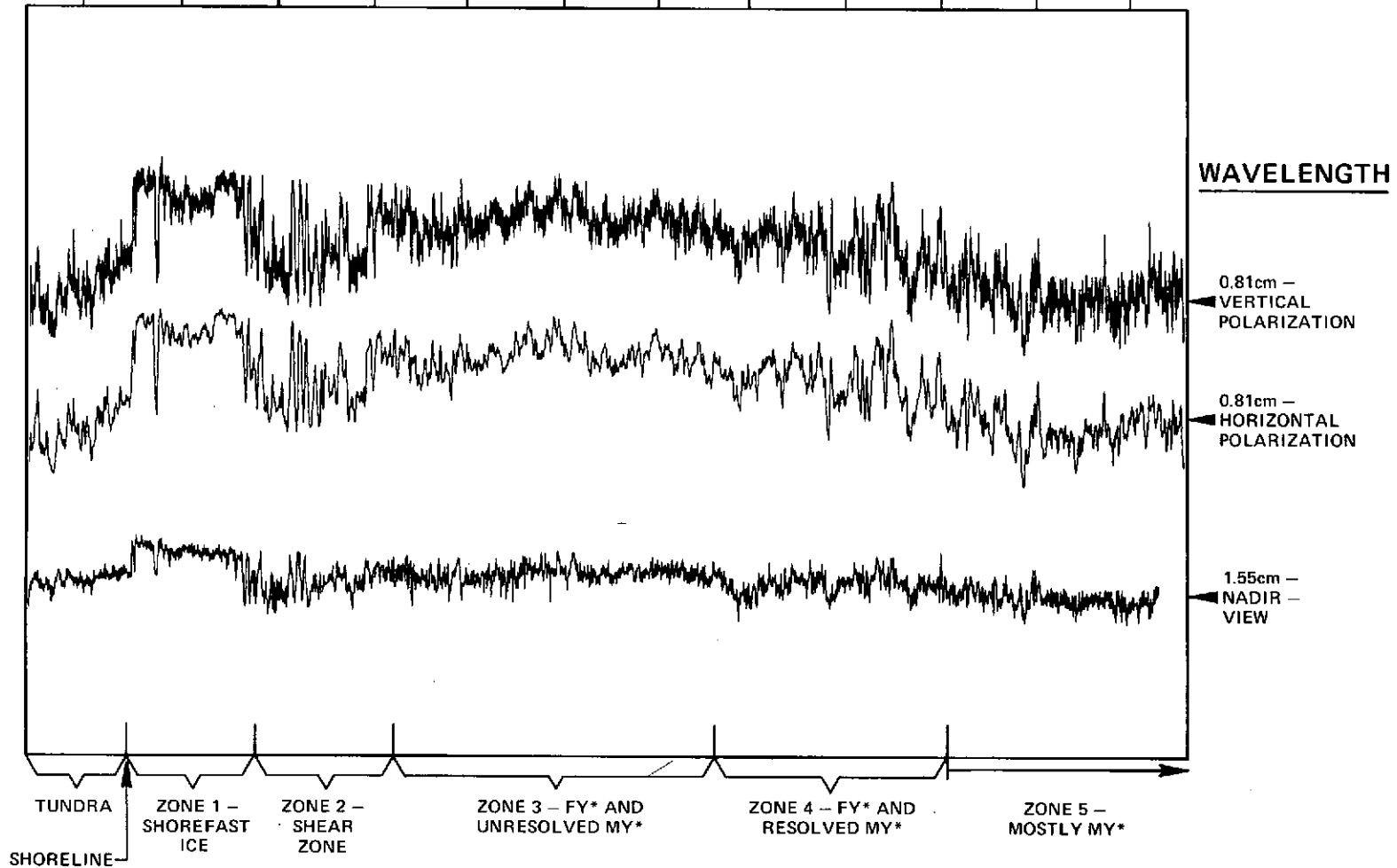
RELATIVE BRIGHTNESS TEMPERATURE



50 °K



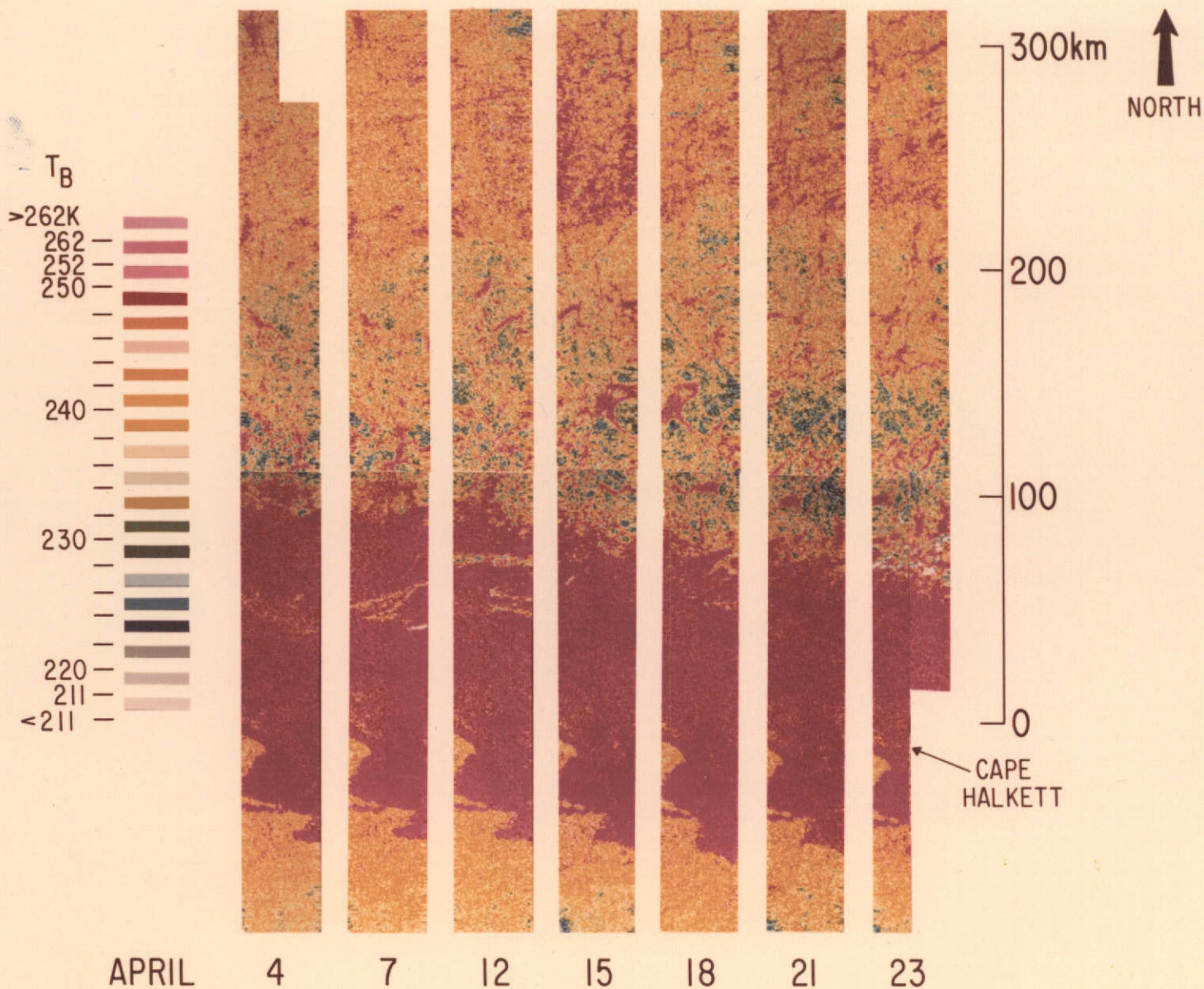
PRECEDING PAGE BLANK NOT FILMED



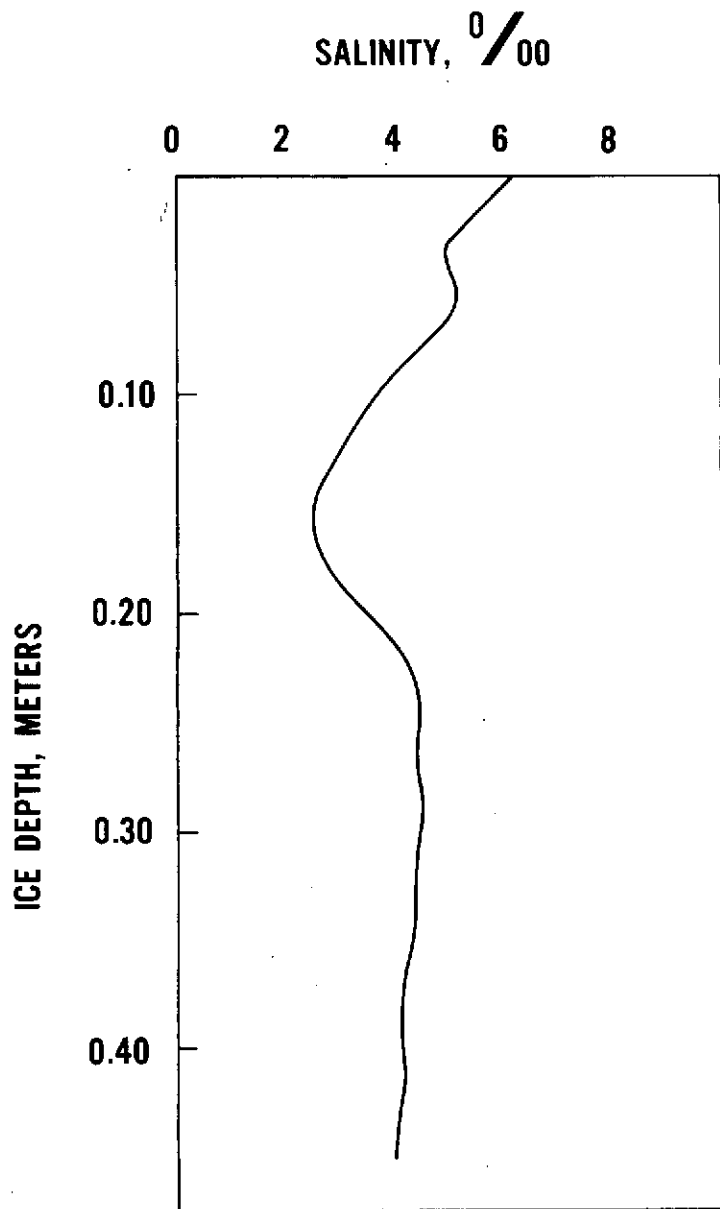
\*FY = FIRST-YEAR SEA ICE  
MY = MULTIYEAR SEA ICE

ARCTIC SEA  
ICE MOTION  
(1972)  
NASA CV-990  
AIRCRAFT  
( $\lambda=1.55\text{cm}$ )

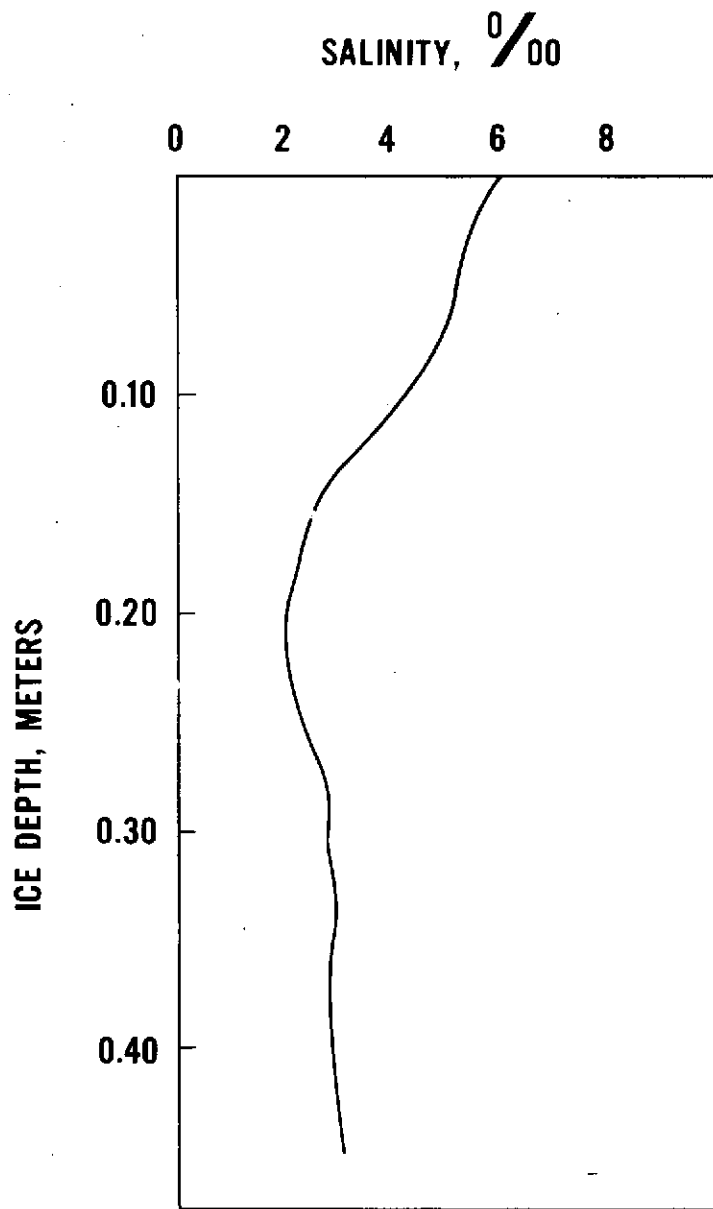
ORIGINAL PAGE IS  
OF POOR QUALITY



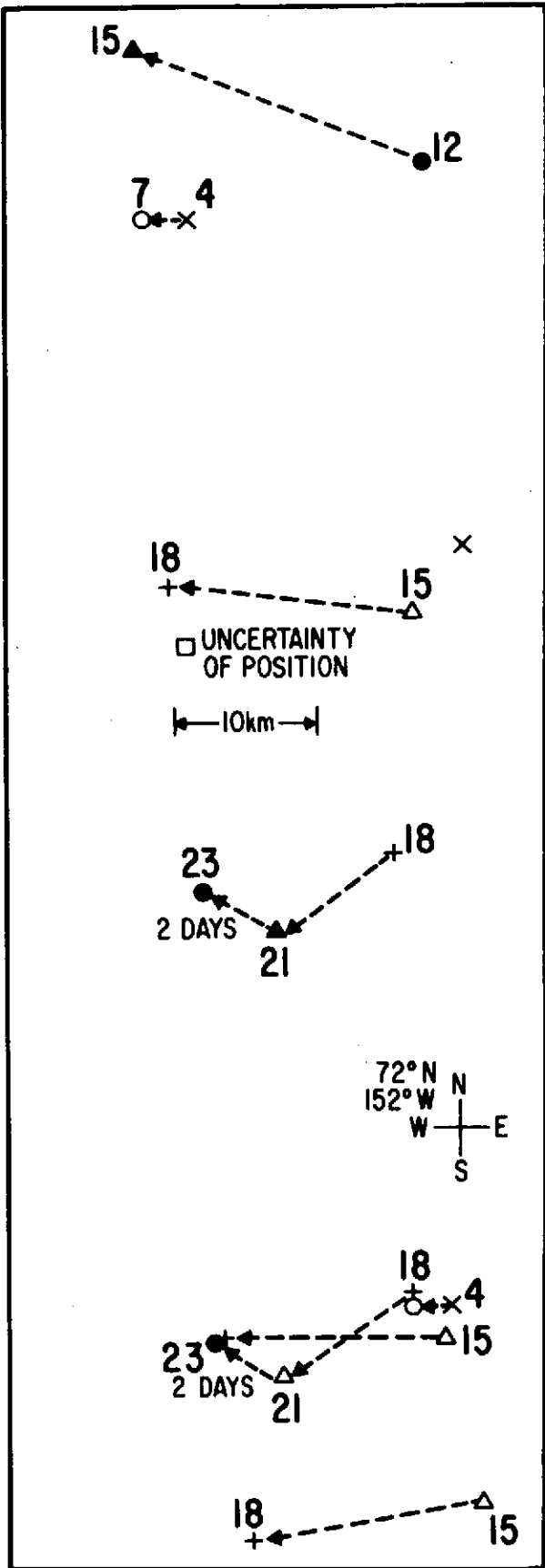
a. HARRISON BAY 26 APRIL 1972



b. KOGRU RIVER 26 APRIL 1972

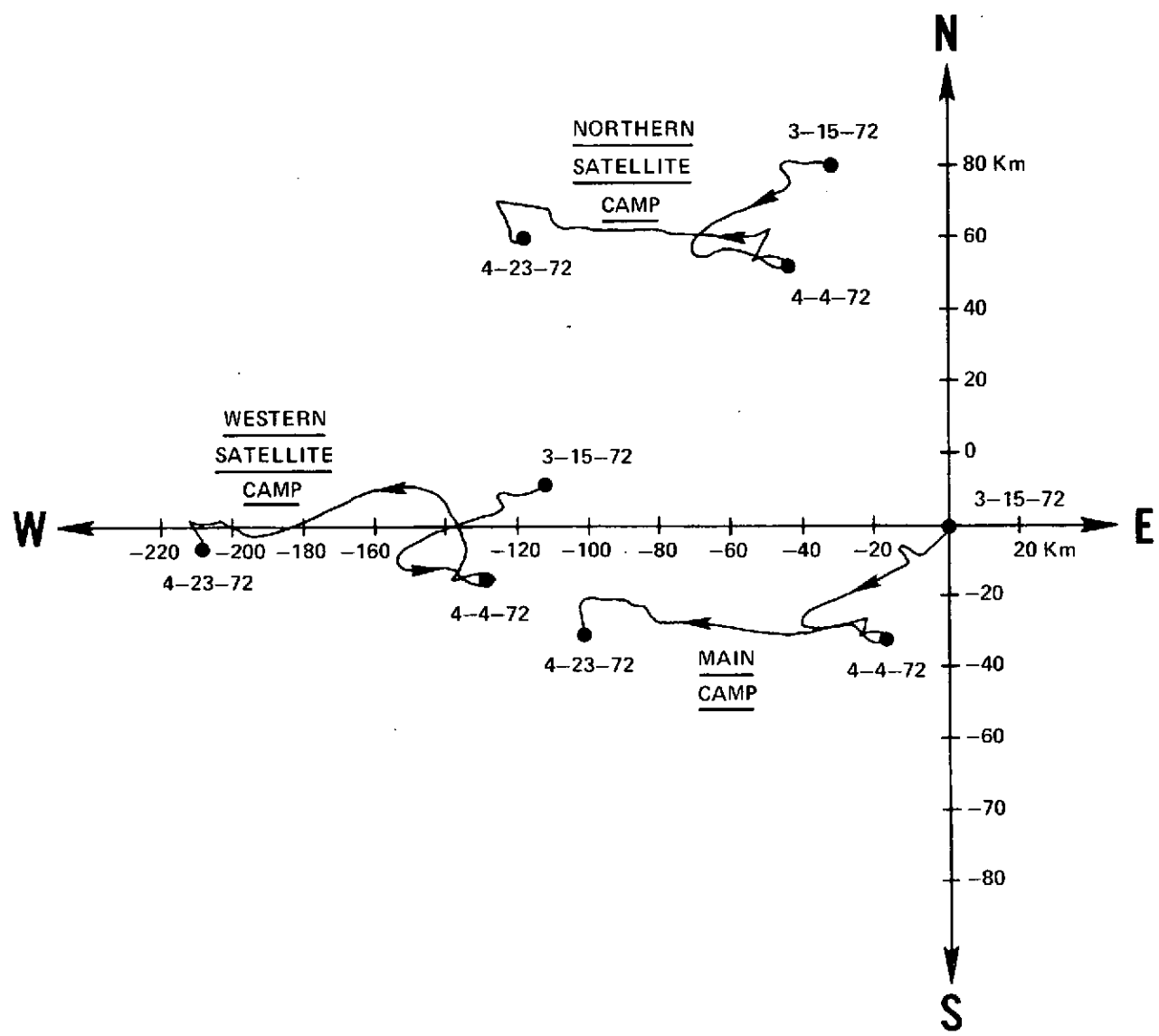


# COMPOSITE OF MOTION IN SHORELINE STRIPS



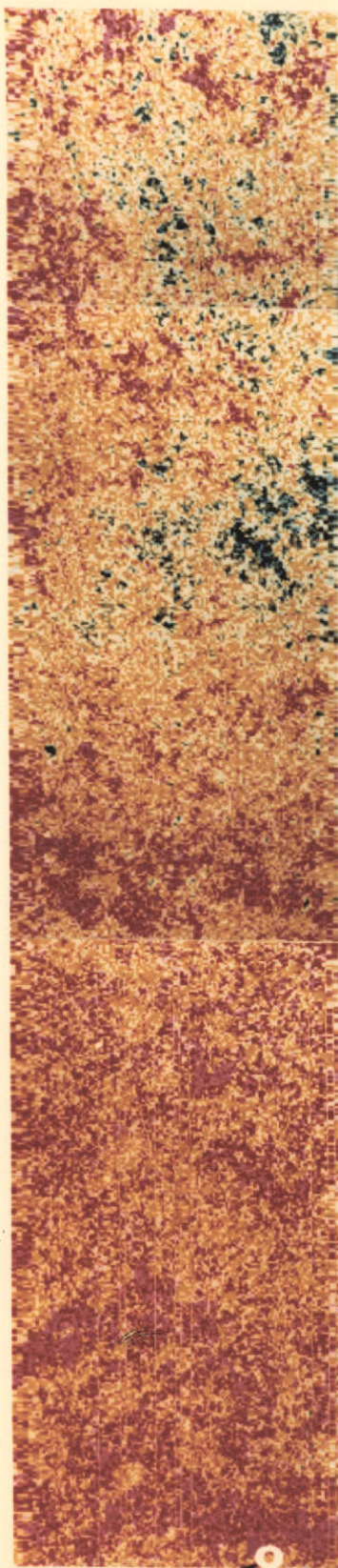


# DRIFT OF STATIONS DURING AIDJEX 1972



151°W

151°W

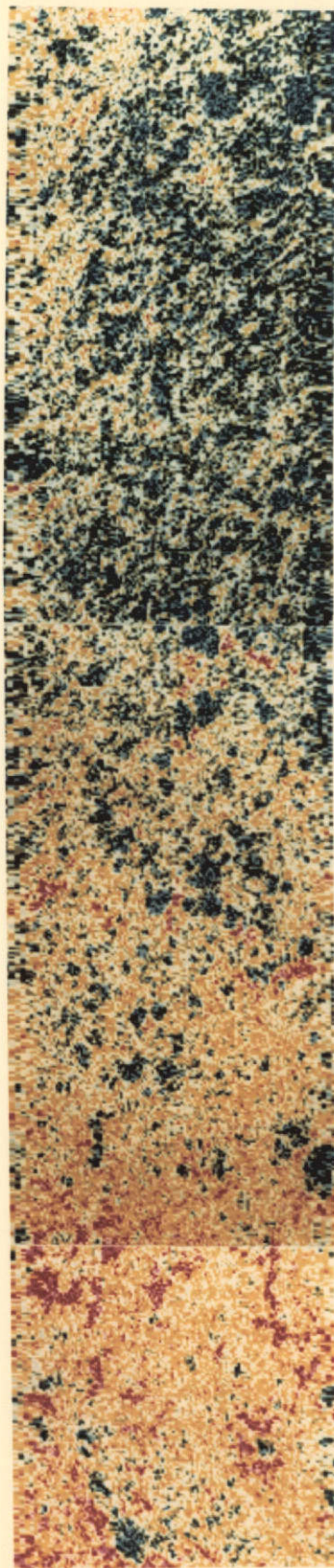


— 77N

— 76N

— 75N

**ORIGINAL PAGE IS  
OF POOR QUALITY**



— 80N

— 79N

— 78N

TIME : FROM 345 06 30 TO 347 19 41 '73

